

Asteroseismology of OB stars

From birth to adulthood

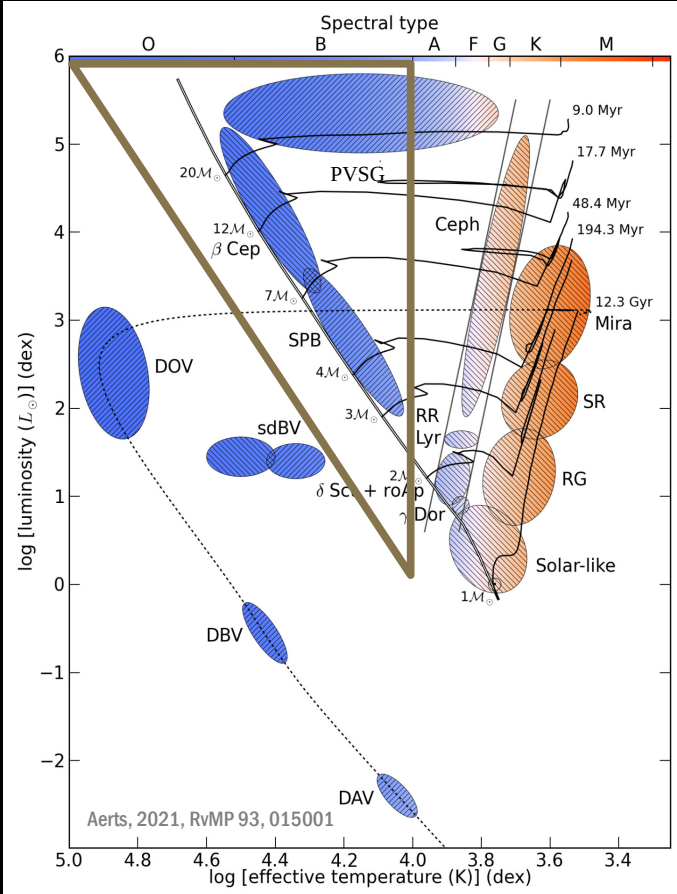
Peter De Cat

Royal Observatory of Belgium, Ringlaan 3, B-1180 Brussels, Belgium

... a very incomplete point of view

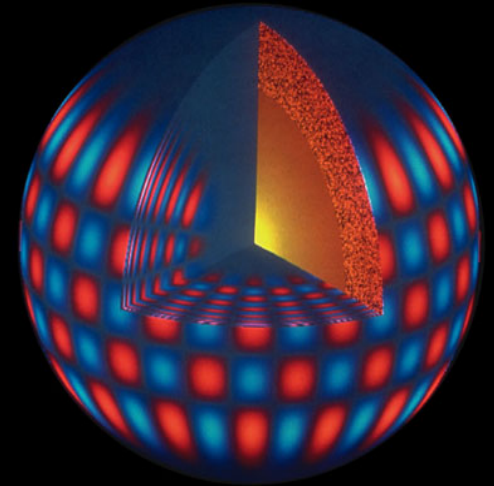
OB-type stars

Convective core
Radiative envelope



- β Cephei stars (β Cep)
 - Low order p and g modes with periods of few hours
- Slowly Pulsating B stars (SPB)
 - High order g modes with periods of several hours to few days
- Periodic Variable Supergiants (PVSG)
 - g modes with periods of order of 10 to 100 days
- Be stars (Be)
 - Rotational modulation and/or Pulsations?
- Maia variables

Hybrids?



Excitation mechanisms at play

- Opacity mechanism operating in Z bump

Period p or Frequency ν

Order n

→ # nodesurfaces in interior

Degree ℓ

→ # nodelines on surface

Azimuthal number m

→ # nodelines on surface \perp equator

Peter De Cat (Royal Observatory of Belgium, Ringlaan 3, B-1180 Brussels, Belgium)

Group meeting at BNU (25/09/2024, Beijing, China)

Asteroseismic requirements and tools

→ Time series

→ Observed pulsation modes

➤ Frequency ν → Frequency analysis

➤ Degree ℓ

➤ Azimuthal number m



Mode identification

* Multicolour photometry:

* High-resolution spectroscopy

mmag precision

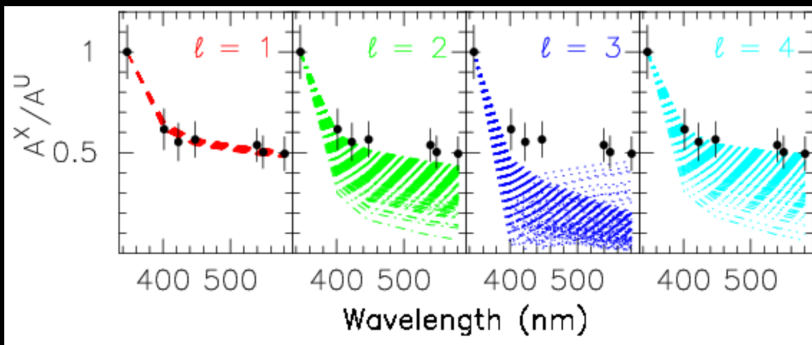
method of photometric amplitude ratios and frequency shifts (Dupret et al., 2003, A&A 398, 677)

HD24587 = 33 Eridani

#137 Geneva photometry

#65 CAT spectra

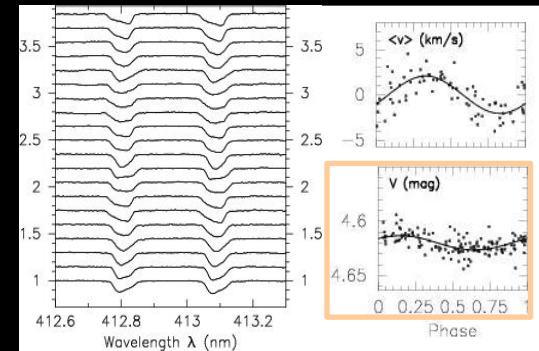
$\nu_1 = 1.1569 \text{ d}^{-1}$



observed amplitude ratios relative to the bluest filter
(given with dots and error bars in black)



compare with calculated amplitude ratios for modes
with different ℓ values
(given with coloured lines)



Asteroseismic requirements and tools

→ Time series

→ Observed pulsation modes

➤ Frequency ν → Frequency analysis

➤ Degree ℓ

➤ Azimuthal number m



Mode identification

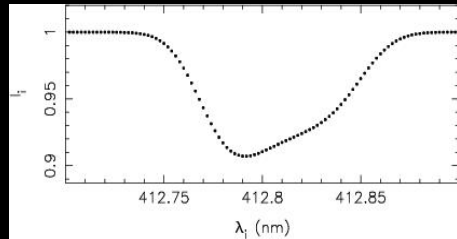
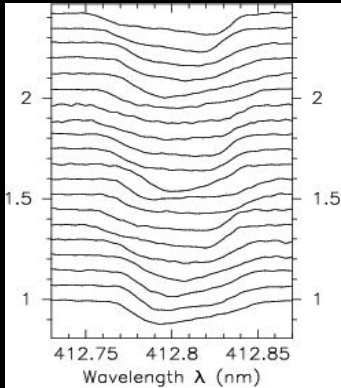
* Multicolour photometry:

* High-resolution spectroscopy: **moment method**

mmag precision

method of photometric amplitude ratios and frequency shifts (Dupret et al., 2003, A&A 398, 677)

(Aerts, 1992, A&A 266, 294; Briquet & Aerts, 2003, A&A 398, 687)

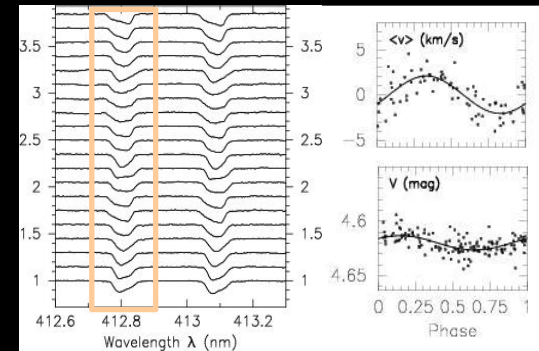


HD24587 = 33 Eridani

#137 Geneva photometry

#65 CAT spectra

$\nu_1 = 1.1569 \text{ d}^{-1}$



Asteroseismic requirements and tools

→ Time series

→ Observed pulsation modes

➤ Frequency f → Frequency analysis

➤ Degree ℓ

➤ Azimuthal number m



Mode identification

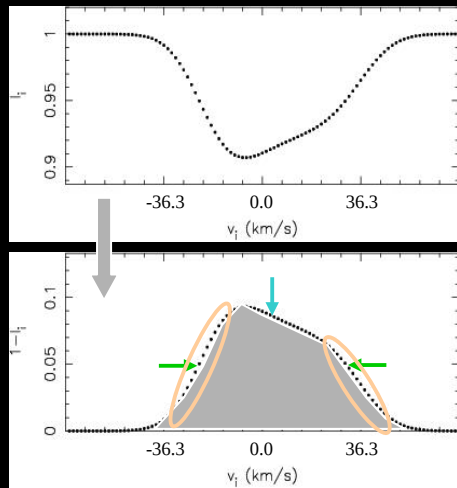
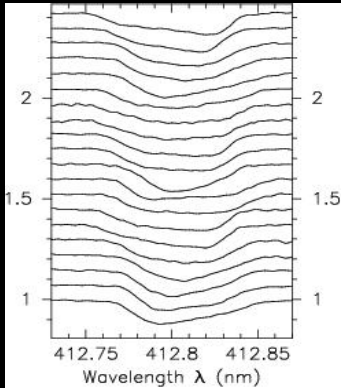
* Multicolour photometry:

* High-resolution spectroscopy: **moment method**

mmag precision

method of photometric amplitude ratios and frequency shifts (Dupret et al., 2003, A&A 398, 677)

(Aerts, 1992, A&A 266, 294; Briquet & Aerts, 2003, A&A 398, 687)



$$\langle v^n \rangle = \frac{\sum_i (1-I_i) v_i^n (v_i - v_{i-1})}{\sum_i (1-I_i) (v_i - v_{i-1})}$$

denominator = equivalent width

$\langle v \rangle$ ~ radial velocity

$\langle v^2 \rangle$ ~ width

$\langle v^3 \rangle$ ~ skewness



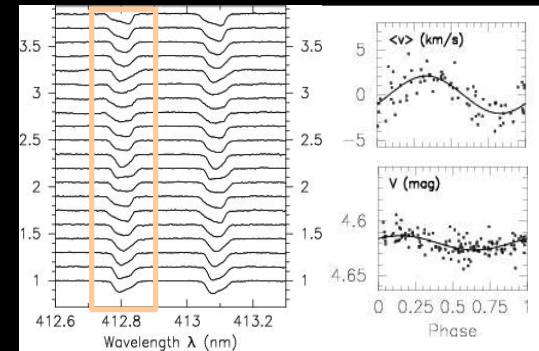
compare with velocity moments
calculated for modes with different (ℓ, m)

HD24587 = 33 Eridani

#137 Geneva photometry

#65 CAT spectra

$\delta_1 = 1.1569 \text{ d}^{-1}$



Asteroseismic requirements and tools

→ Time series

→ Observed pulsation modes

➤ Frequency ν → Frequency analysis

➤ Degree ℓ

➤ Azimuthal number m



Mode identification

* Multicolour photometry:

* High-resolution spectroscopy:

mmag precision

method of photometric amplitude ratios and frequency shifts (Dupret et al., 2003, A&A 398, 677)

moment method (Aerts, 1992, A&A 266, 294; Briquet & Aerts, 2003, A&A 398, 687)

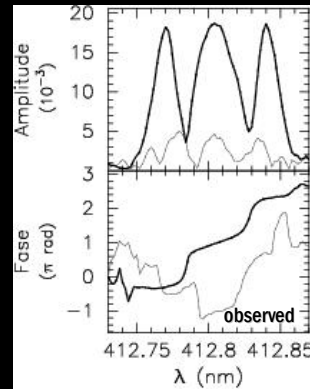
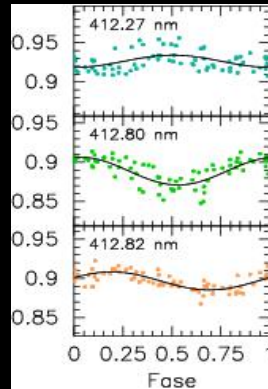
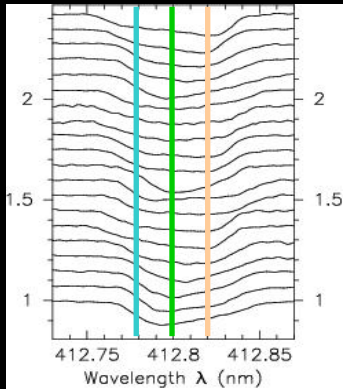
fourier parameter fit method (Zima, 2006, A&A 455, 227)

HD24587 = 33 Eridani

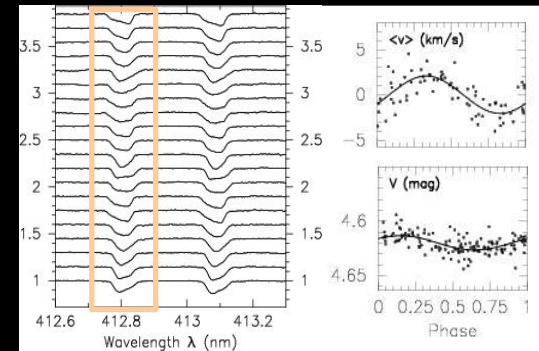
#137 Geneva phometry

#65 CAT spectra

$\nu_1 = 1.1569 \text{ d}^{-1}$



change of amplitude and phase within observed line profiles ⇒ compare with those calculated for modes with different (ℓ, m)



Asteroseismic requirements and tools

→ Time series

→ Observed pulsation modes

➤ Frequency f → Frequency analysis

➤ Degree l

➤ Azimuthal number m

↓
Modelling

Mode identification

* Multicolour photometry:

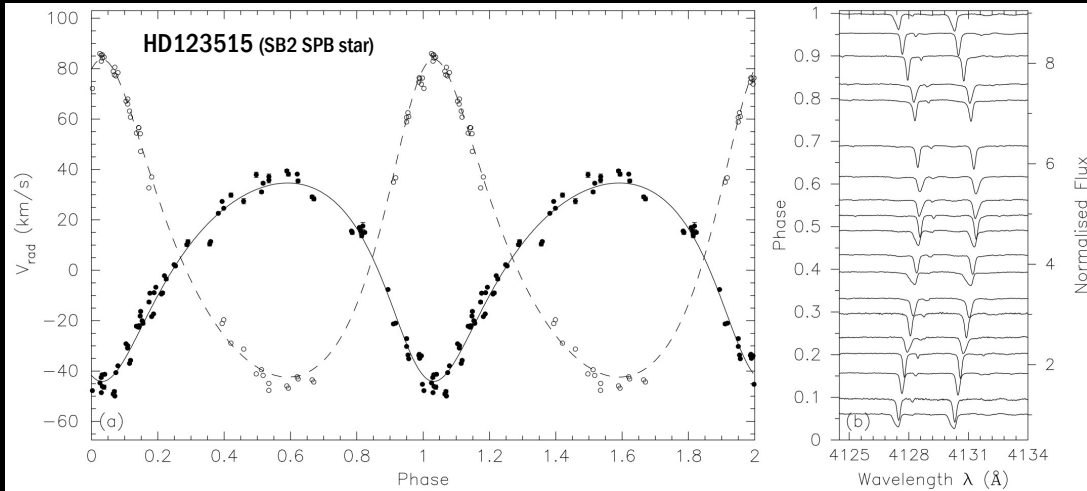
* High-resolution spectroscopy:

mmag precision

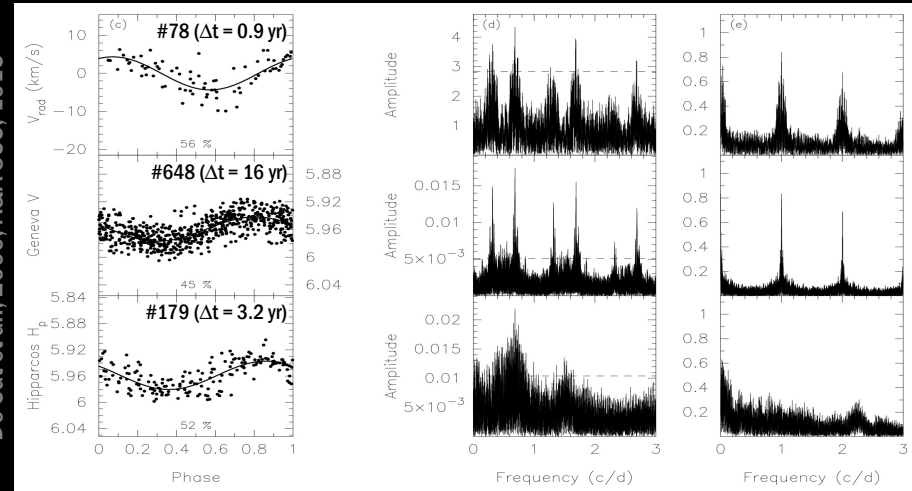
method of photometric amplitude ratios and frequency shifts (Dupret et al., 2003, A&A 398, 677)

moment method (Aerts, 1992, A&A 266, 294; Briquet & Aerts, 2003, A&A 398, 687)

fourier parameter fit method (Zima, 2006, A&A 455, 227)



De Cat et al., 2000, A&A 355, 1015



Asteroseismic requirements and tools

→ Time series

→ Observed pulsation modes

➤ Frequency f → Frequency analysis

➤ Degree l } Mode identification

➤ Azimuthal number m }

↓
Modelling

μmag precision

* Multicolour photometry:

method of photometric amplitude ratios and frequency shifts (Dupret et al., 2003, A&A 398, 677)

* High-resolution spectroscopy:

moment method (Aerts, 1992, A&A 266, 294; Briquet & Aerts, 2003, A&A 398, 687)

fourier parameter fit method (Zima, 2006, A&A 455, 227)

2003-2019



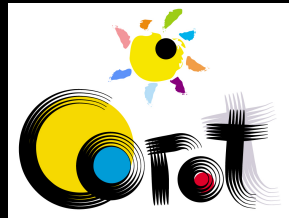
2009-2018



2018-now



2006-2014



2013-now



2013-now



Gaia

Asteroseismic requirements and tools

→ Time series

→ Observed pulsation modes

➤ Frequency f → Frequency analysis

➤ Degree ℓ

➤ Azimuthal number m

↓
Modelling

Mode identification

* Multicolour photometry:

* High-resolution spectroscopy:

μmag precision

method of photometric amplitude ratios and frequency shifts (Dupret et al., 2003, A&A 398, 677)

moment method (Aerts, 1992, A&A 266, 294; Briquet & Aerts, 2003, A&A 398, 687)

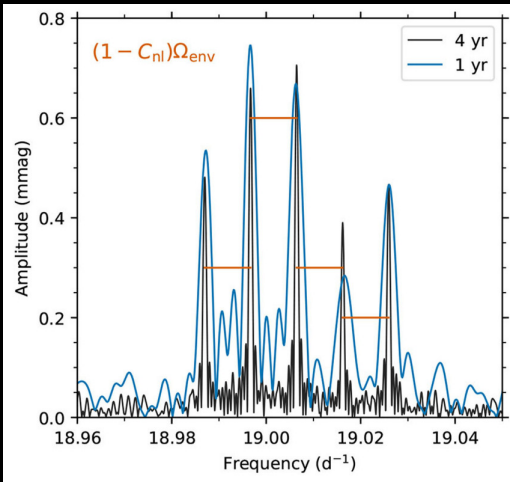
fourier parameter fit method (Zima, 2006, A&A 455, 227)

→ Present day asteroseismic diagnostics

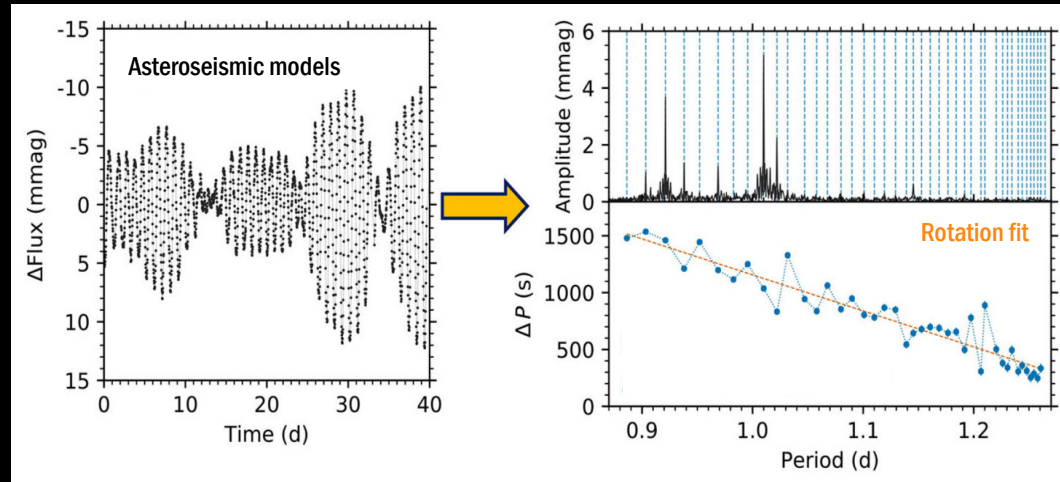
➤ Rotational multiplets

➤ g mode period spacing patterns (asymptotic regime)

Bowman, 2020, FrASS 7, 70



Bowman, 2020, FrASS 7, 70



Asteroseismic requirements and tools

→ Time series

→ Observed pulsation modes

➤ Frequency f → Frequency analysis

➤ Degree ℓ } Mode identification

➤ Azimuthal number m }

↓
Modelling

* Multicolour photometry: μ mag precision

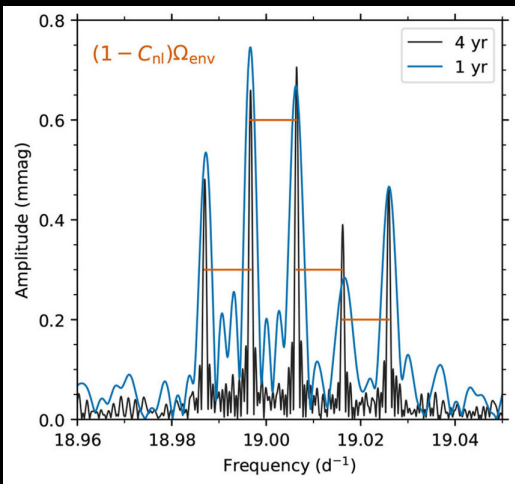
* High-resolution spectroscopy: moment method (Aerts, 1992, A&A 266, 294; Briquet & Aerts, 2003, A&A 398, 687)
fourier parameter fit method (Zima, 2006, A&A 455, 227)

→ Present day asteroseismic diagnostics

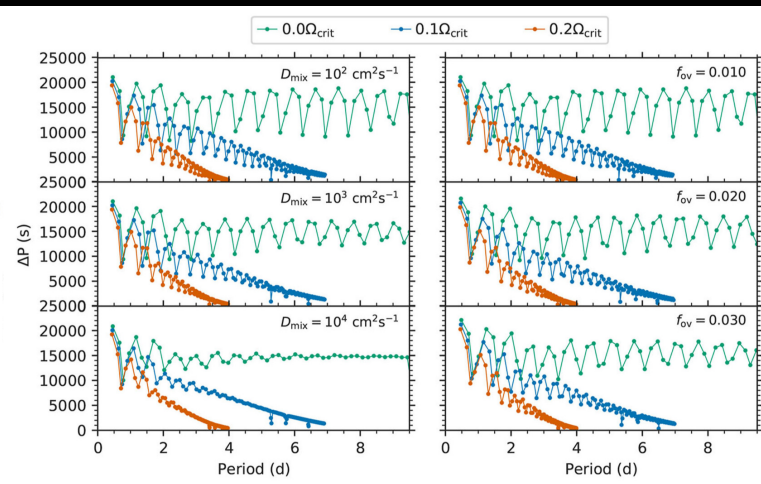
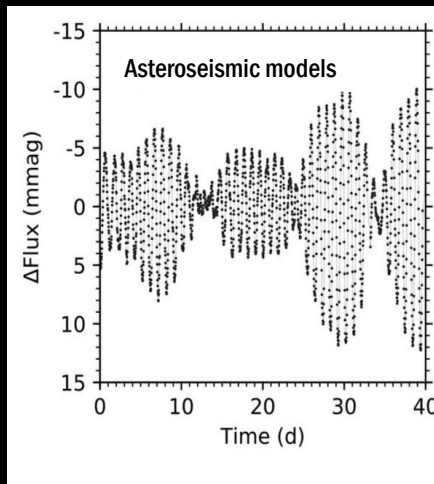
➤ Rotational multiplets

➤ g mode period spacing patterns (asymptotic regime)

Bowman, 2020, FrASS 7, 70



Bowman, 2020, FrASS 7, 70



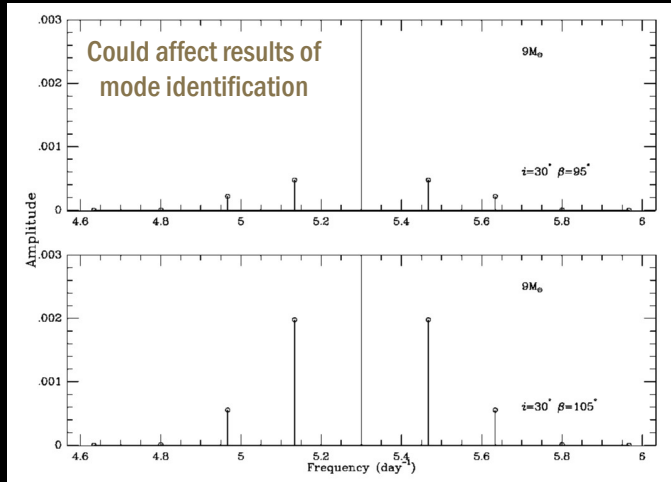
Magnetic fields

Fossil field

→ Effects of magnetic field on asteroseismic diagnostics of pulsating stars

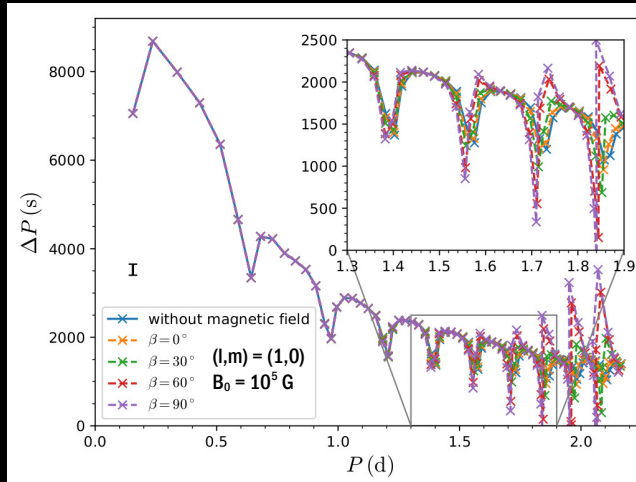
➤ Magnetic multiplets

(Shibahashi & Aerts, 2000, ApJ 531, L143)



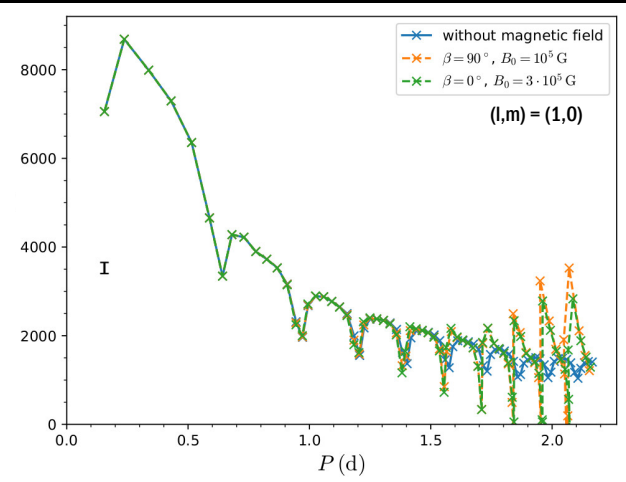
➤ Period spacings

(Prat et al., 2020, A&A 636, A100)



➤ Inhibition of mixing ⇒ no overshooting

(Briquet et al., 2016, A&A 587, A126)



Magneto-asteroseismology

✓ Ground-based

β Cep

(Shibahashi & Aerts, 2000, ApJ 531, L143)

ζ Cas

(Briquet et al., 2016, A&A 587, A126)

V2052 Oph

(Briquet et al., 2012, MNRAS 427, 483)

✓ CoRoT

HD43317

(Buysschaert et al., 2018, A&A 616, A148)

✓ K2

ι Lib

(Buysschaert et al., 2018, SF2A Conf., 369)

Peter De Cat (Royal Observatory of Belgium, Ringlaan 3, B-1180 Brussels, Belgium)

Group meeting at BNU (25/09/2024, Beijing, China)

→ Overview of surveys to (1) discover new magnetic massive stars with spectropolarimetric observations
(2) improve the models of magnetic stars

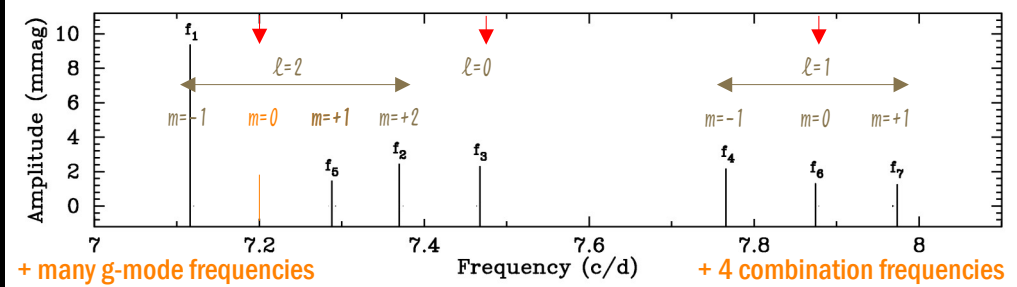
- **BOB** B Fields in OB Stars (Morel et al., 2014, Messenger 157, 27)
 - ✓ Southern OB stars
- **BritePol** BRITE spectropolarimetric survey (Neiner et al., 2014, SF2A Conf, 505)
 - ✓ ~600 stars with $V \leq 4$
- **BinaMIcs** Binarity and Magnetic Interactions in various classes of stars (Alecian et al., 2015, IAUS 307, 330)
 - ✓ ~200 hot binary stars
- **MiMeS** Magnetism in Massive Stars (Wade et al., 2016, MNRAS 456, 2)
 - ✓ ~550 massive stars
- **LIFE** Large Impact of magnetic Fields on the Evolution of hot stars (Martin et al., 2018, MNRAS 475, 1521)
 - ✓ ~60 evolved hot stars
- **MOBSTER** Magnetic OB[A] Stars with TESS: probing their Evolutionary and Rotational properties (David-Uraz et al., 2019, MNRAS 487, 304)
 - ✓ confirmed and candidate magnetic OBA stars that are observed with TESS

Detected for ~10% of B stars

Opacities

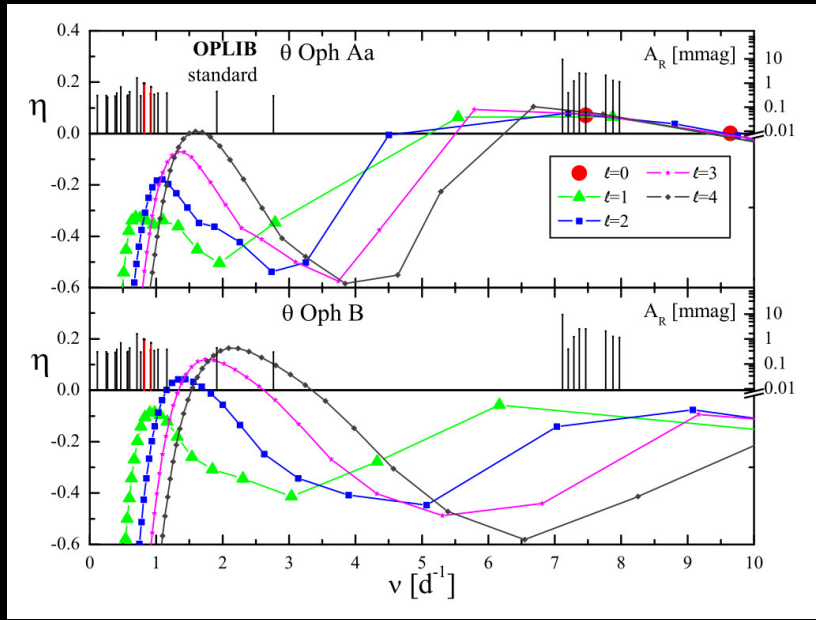
→ θ Ophiuchi (Walczak et al., 2019, MNRAS 485, 3544)

- Known β Cep pulsator with 7 pulsation frequencies Hybrid pulsator
 - Triple system:
 - ✓ θ Oph Aa: massive B2IV star
 - ✓ θ Oph Ab: low-mass star ($M < 1 M_{\odot}$)
 - ✓ θ Oph B: massive B5 star
- } 56.71 days } ~ 14 years



BRITE photometry (2014 UBr; 2016+2017 UBr, BHr, BAB, BLb)
SMEI photometry (2003-2010)

Driving }
Damping }



- Complex asteroseismology
 - ✓ Fitting centroid frequencies
 - ✓ Getting the mode instability in the observed frequency range
 - ✓ Reproduce the empirical value of f (ratio of the relative bolometric flux to the relative radial displacement)



Opacities

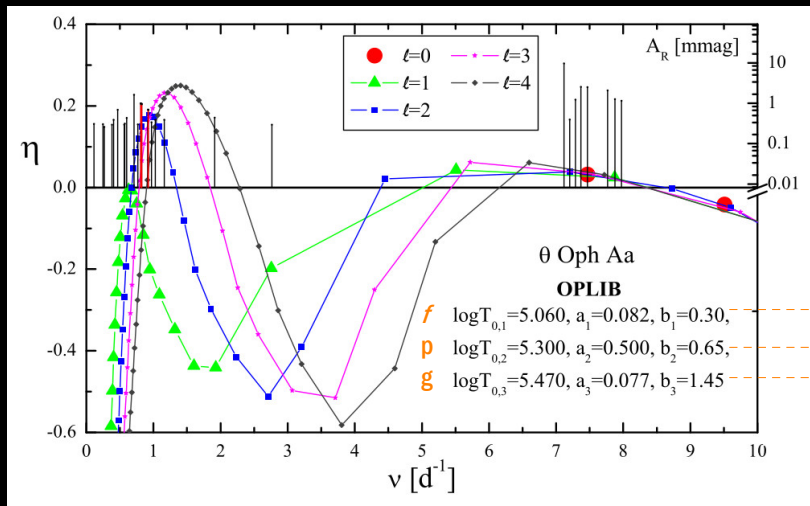
→ θ Ophiuchi (Walczak et al., 2019, MNRAS 485, 3544)

➤ Known β Cep pulsator with 7 pulsation frequencies

Hybrid pulsator

➤ Triple system:

- ✓ θ Oph Aa: massive B2IV star
 - ✓ θ Oph Ab: low-mass star ($M < 1 M_{\odot}$)
 - ✓ θ Oph B: massive B5 star
- } 56.71 days } ~ 14 years



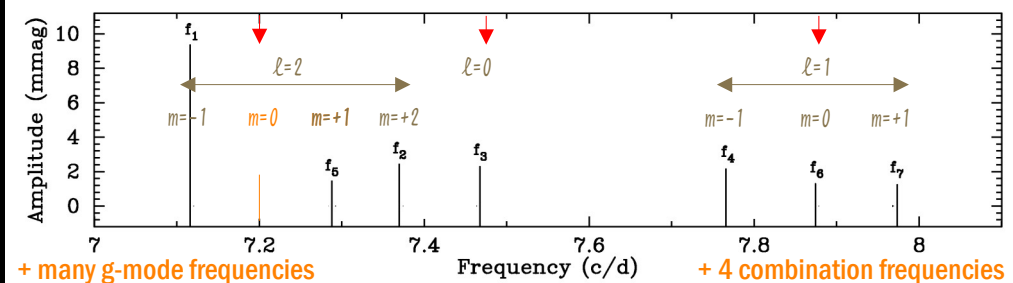
➤ Complex asteroseismology

- ✓ Fitting centroid frequencies
- ✓ Getting the mode instability in the observed frequency range
- ✓ Reproduce the empirical value of f (ratio of the relative bolometric flux to the relative radial displacement)

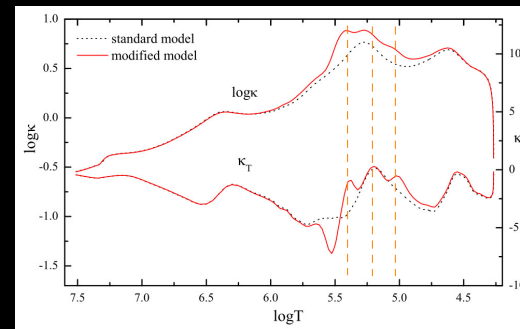
— Kurucz bump

— Z-bump

— Ni



BRITE photometry (2014 UBr; 2016+2017 UBr, BHR, BAB, BLb)
SMEI photometry (2003-2010)

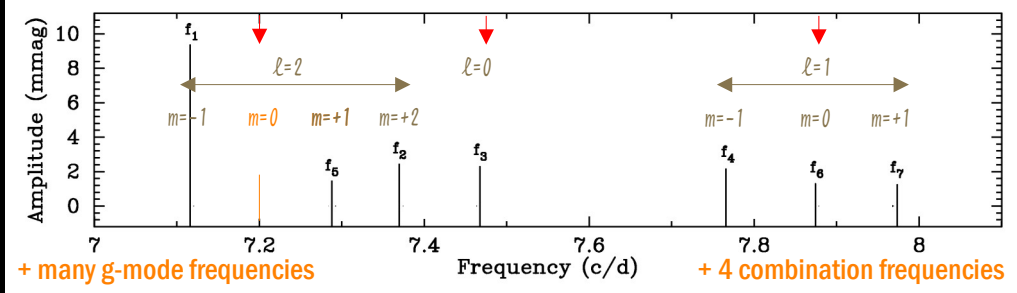
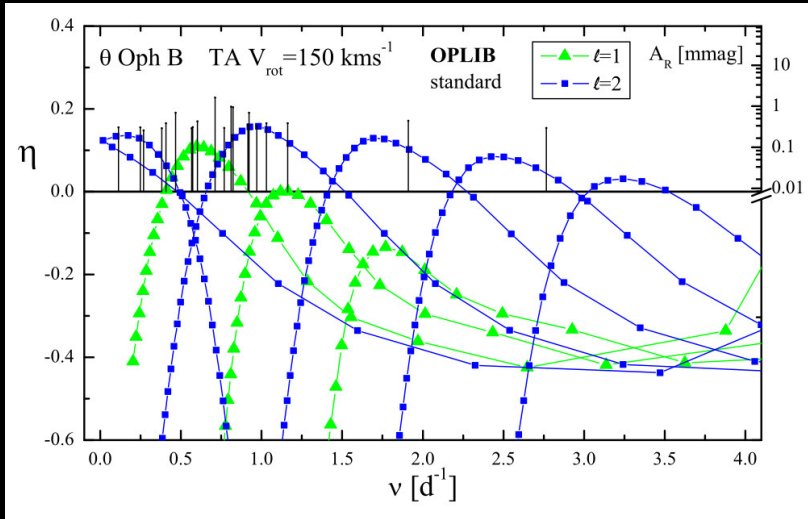


Opacity increase
needed to excite g-
modes
(θ Oph Aa)

Opacities

→ θ Ophiuchi (Walczak et al., 2019, MNRAS 485, 3544)

- Known β Cep pulsator with 7 pulsation frequencies Hybrid pulsator
 - Triple system:
 - ✓ θ Oph Aa: massive B2IV star
 - ✓ θ Oph Ab: low-mass star ($M < 1 M_{\odot}$)
 - ✓ θ Oph B: massive B5 star
- $\left. \begin{array}{l} 56.71 \text{ days} \\ \sim 14 \text{ years} \end{array} \right\}$



BRITE photometry (2014 UBr; 2016+2017 UBr, BHR, BAB, BLb)
SMEI photometry (2003-2010)

- Complex asteroseismology
 - ✓ Fitting centroid frequencies
 - ✓ Getting the mode instability in the observed frequency range
 - ✓ Reproduce the empirical value of f (ratio of the relative bolometric flux to the relative radial displacement)

Fast rotation
needed to excite g-
modes
(θ Oph B)

Opacity increase
needed to excite g-
modes
(θ Oph Aa)

Opacities

→ θ Ophiuchi (Walczak et al., 2019, MNRAS 485, 3544)

→ β Centauri (Pigulski et al., 2016, A&A 588, A55)

➤ Triple system:

- ✓ β Cen Aa: early B-type star ($M = 12.02(13) M_{\odot}$), faster rotator ($v_{\text{rot}} = 200\text{-}250 \text{ km s}^{-1}$)
- ✓ β Cen Ab: early B-type star ($M = 10.58(18) M_{\odot}$), slower rotator ($v_{\text{rot}} = 70\text{-}120 \text{ km s}^{-1}$)
- ✓ β Cen B: distant, mid B-type star

➤ 8 g-modes, 9 p-modes, and 2 combination frequencies

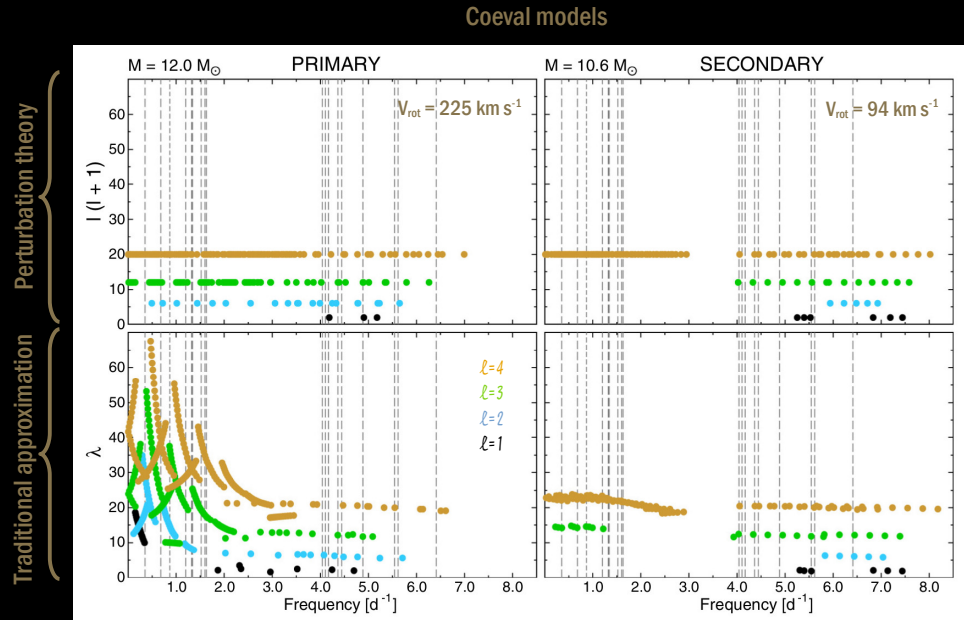
Light time effect: attribution to Aa and Ab component inconclusive for most frequencies

If effects rotation
taken into account,
no need for
Increase opacity
Increase metallicity
Change chemical composition

Ideal to study influence of
Rotation Magnetic field

357 days
 $e=0.81$
magnetic resolved } 125-220 years

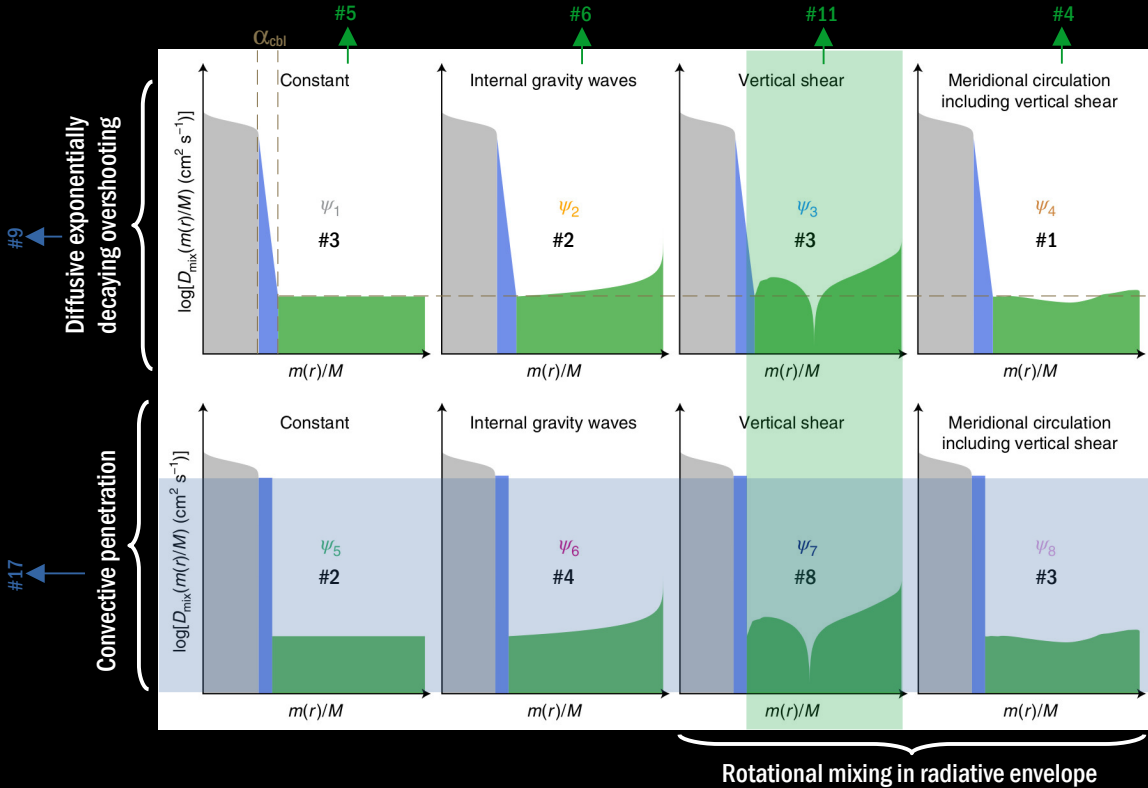
BRITE photometry (2014, 146d, UBr, BTr, BAb, BLb)
BRITE photometry (2014, 27d, BLb)
BRITE photometry (2014, 6d, BTr)



Interior mixing profile

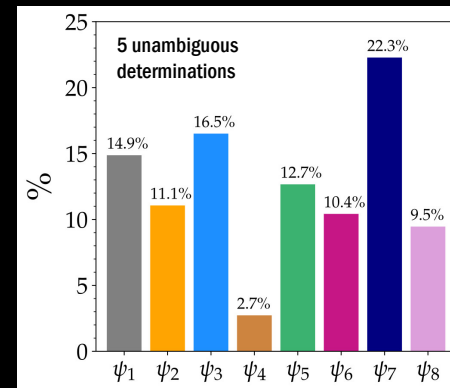
→ Pedersen et al., 2021, NatAs 5, 715

- Sample of 26 SPB stars showing period spacings patterns from dipole g-modes (~4% of all B stars in the nominal Kepler field of view)
- Asteroseismic modelling with eight different interior mixing profiles $D_{\text{mix}}(r)$ each having three regions (convective core $D_{\text{com}}(r)$, core boundary layer $D_{\text{cbl}}(r)$, radiative envelope $D_{\text{env}}(r)$)



- M_{ini} initial mass
- Z metal mass fraction
- X_c/X_{ini} hydrogen mass fraction in fully mixed convective core/initial hydrogen mass fraction
- Ω_{rot} interior rotation frequency
- α_{cbl} length scale connected with the size of the core boundary layer
- $D_{\text{env},0}$ level of mixing at bottom of radiative envelope

Majority for convective penetration (55%)
vertical shear (39%)



Pedersen, 2022, AJ 930, 94

- Expected helium core masses at end of main-sequence evolution:
 - * underestimated without mixing
 - * increase with initial stellar mass
 - * heavily influenced by amount of envelope mixing

cf. Kaiser et al, 2020, MNRAS 496, 1967
Johnston, 2021, A&A 655, A29

Peter De Cat (Royal Observatory of Belgium, Ringlaan 3, B-1180 Brussels, Belgium)

Group meeting at BNU (25/09/2024, Beijing, China)

Interior rotation profile

→ HD201433 (Kallinger et al., 2017, A&A 603, A13)

➤ Single-lined spectroscopic triple system:

- ✓ B9V star (suspected SPB star; close to the cool border of instability strip) with two low mass companions
- ✓ 3.3 days
- ✓ 154 days

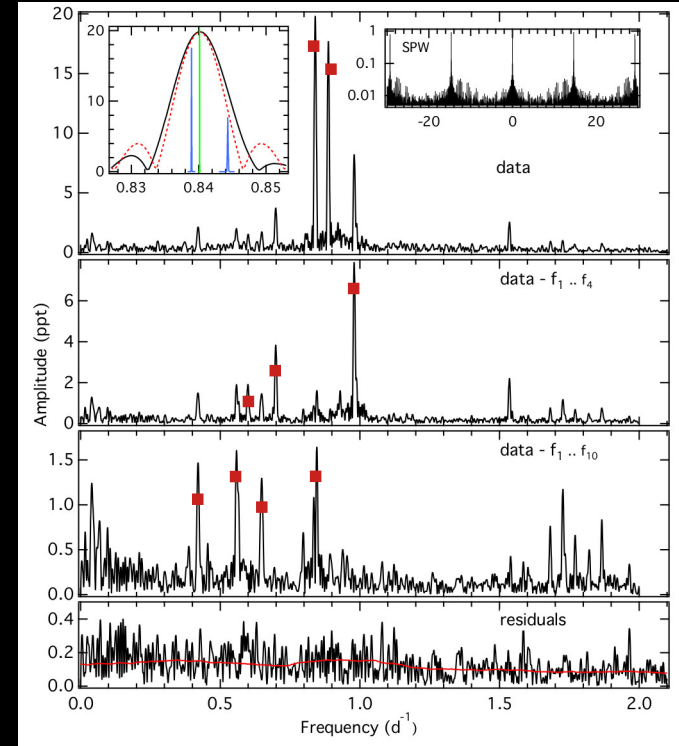
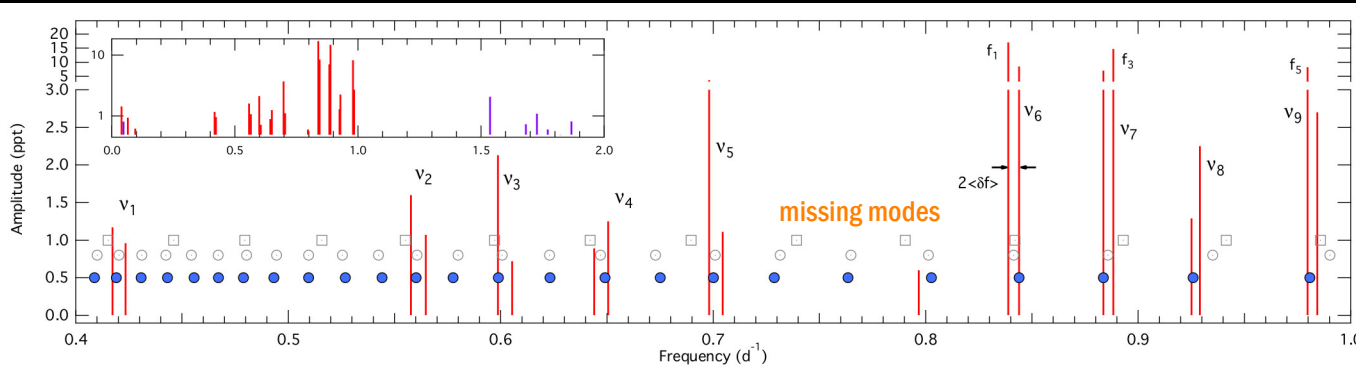
➤ Frequency analysis BTr data

- ✓ 9 statistically significant closely separated doublets ($\ell=1$ modes with $m=\pm 1$) (red squares)
- ✓ 4 additional independent frequencies
- ✓ 7 combination frequencies

BRITE photometry (6 seasons in 2013-2019; 156 days; BTr, Blb; cadence 0.338 min)

SMEI photometry (8 years; 101.6 min)

Radial velocities (96 years)



Interior rotation profile

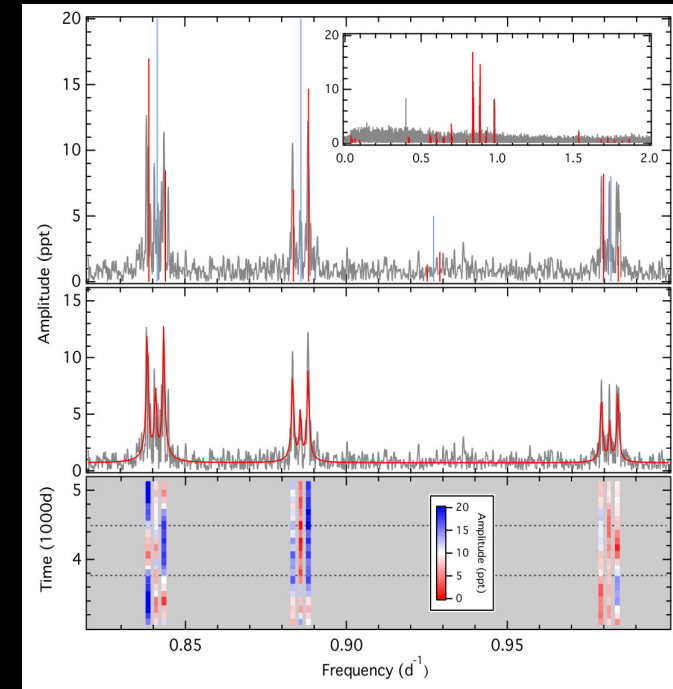
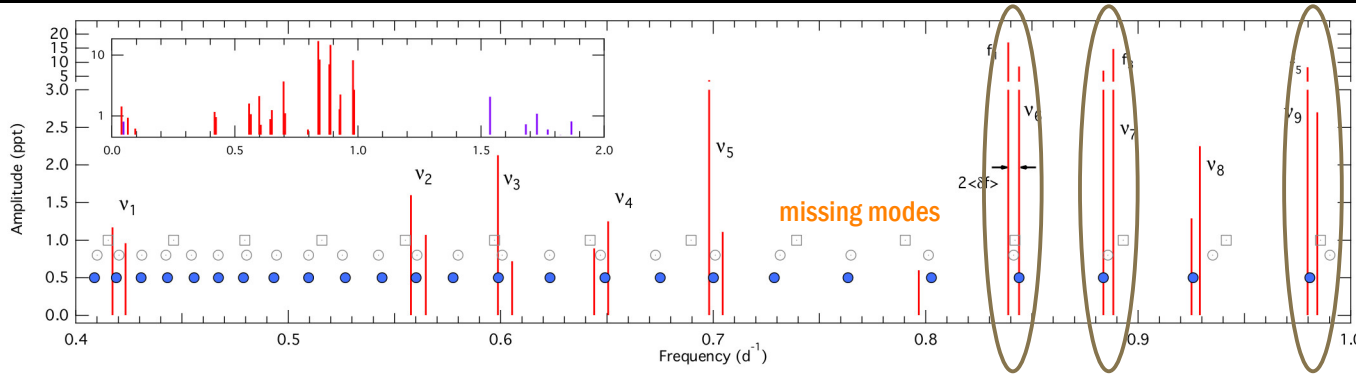
→ HD201433 (Kallinger et al., 2017, A&A 603, A13)

- Single-lined spectroscopic triple system:
 - ✓ B9V star (suspected SPB star; close to the cool border of instability strip) with two low mass companions
 - ✓ 3.3 days
 - ✓ 154 days
- Frequency analysis BTr data
- Frequency analysis SMEI data
 - ✓ Confirmation 3 closely separated triplets of $\ell=1$ modes
 - ✓ Evidence for amplitude changes (mode lifetime of 680(110) days)

BRITE photometry (6 seasons in 2013-2019; 156 days; BTr, Blb; cadence 0.338 min)

SMEI photometry (8 years; 101.6 min)

Radial velocities (96 years)



Peter De Cat (Royal Observatory of Belgium, Ringlaan 3, B-1180 Brussels, Belgium)

Group meeting at BNU (25/09/2024, Beijing, China)

Interior rotation profile

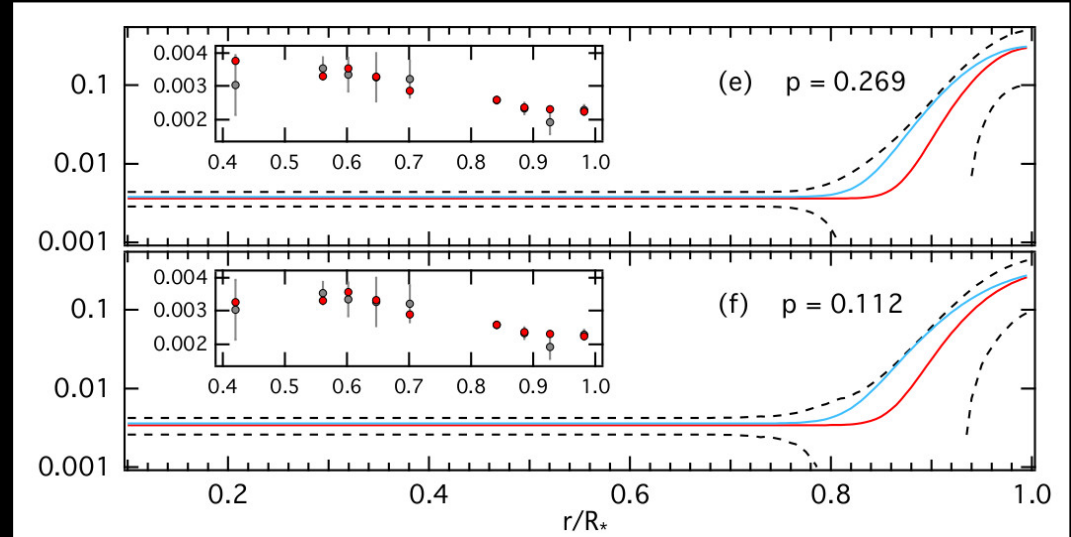
→ HD201433 (Kallinger et al., 2017, A&A 603, A13)

- Single-lined spectroscopic triple system:
 - ✓ B9V star (suspected SPB star; close to the cool border of instability strip) with two low mass companions
 - ✓ 3.3 days
 - ✓ 154 days
- Frequency analysis BTr data
- Frequency analysis SMEI data
- Interior rotation profile radiative envelope
 - ✓ Slowly and rigidly rotating envelope
 - ✓ Thin and significantly more rapidly rotating surface layer
 - ➔ Compatible with orbital period of innermost companion

BRITE photometry (6 seasons in 2013-2019; 156 days; BTr, Blb; cadence 0.338 min)

SMEI photometry (8 years; 101.6 min)

Radial velocities (96 years)



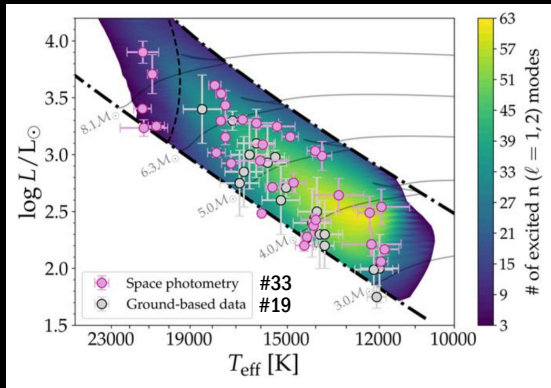
Peter De Cat (Royal Observatory of Belgium, Ringlaan 3, B-1180 Brussels, Belgium)

Group meeting at BNU (25/09/2024, Beijing, China)

Interior rotation profile

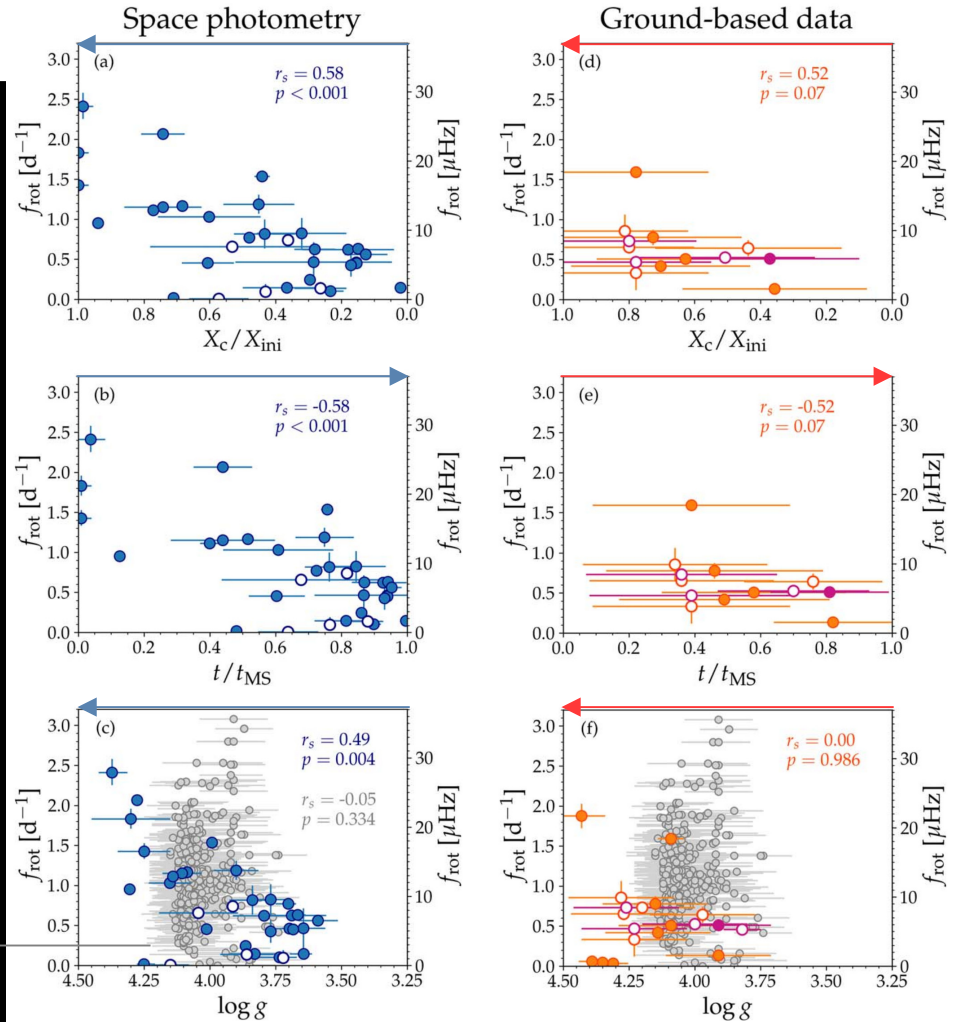
→ Pedersen, 2022, ApJ 940, 49

- 52 SPB stars for which
 - ✓ Internal rotation frequencies derived using g-mode oscillations
 - ✓ Unambiguous mode identification for at least one g-mode
 - ✓ Ages from X_c/X_{ini} , t/t_{MS} and/or $\log g$



Core rotation decreases with age

300 γ Dor stars
(Li et al., 2020, MNRAS 491, 3586)



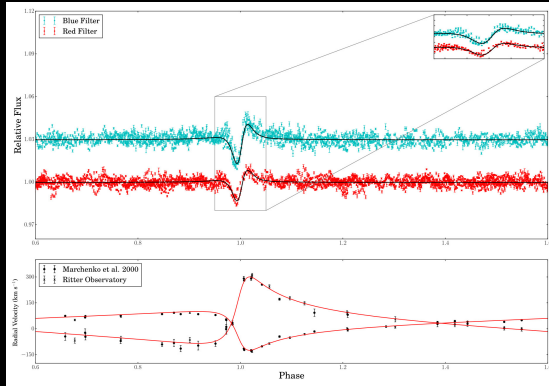
Peter De Cat (Royal Observatory of Belgium, Ringlaan 3, B-1180 Brussels, Belgium)

Group meeting at BNU (25/09/2024, Beijing, China)

Tidal forces

→ ι Orionis (Pablo et al., 2017, MNRAS 467, 2494)

- Massive binary
 - ✓ O9 III + B1 III/IV
 - ✓ $P_{\text{orb}} = 29.13376$ days
 - ✓ $e = 0.764$
- Frequency analysis
 - ✓ 7 frequencies

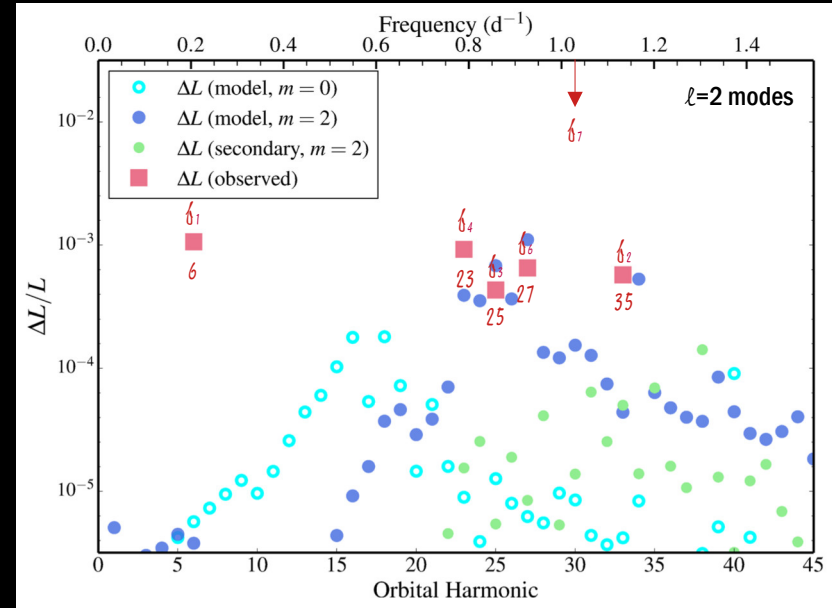


(heartbeat signal at periastron)

→ η Carina (Richardson et al., 2018, MNRAS 475, 5417)

→ ε Lupi (Pablo et al., 2019, MNRAS 488, 64)

BRITE photometry (2013 & 2015; 9 months; UBr, BTr, BHR, BAb, Blb)
 High-resolution spectra (2025-2016; #11; 1.06-m Ritter Observatory)
 Archival radial velocities (Marchenko et al., 2000)



Tidally excited oscillations
 discovered in O stars

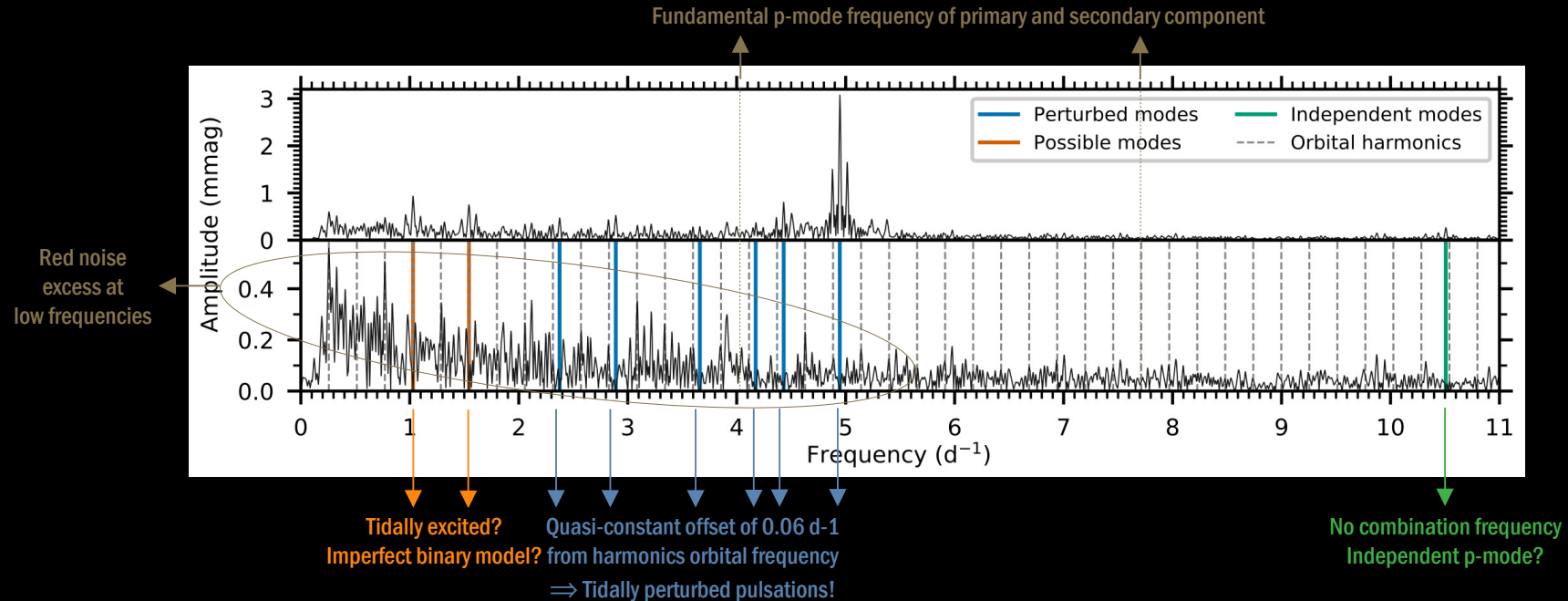
Peter De Cat (Royal Observatory of Belgium, Ringlaan 3, B-1180 Brussels, Belgium)

Group meeting at BNU (25/09/2024, Beijing, China)

Tidal forces

→ V453 Cygni (Southworth et al., 2020, MNRAS 497, L19)

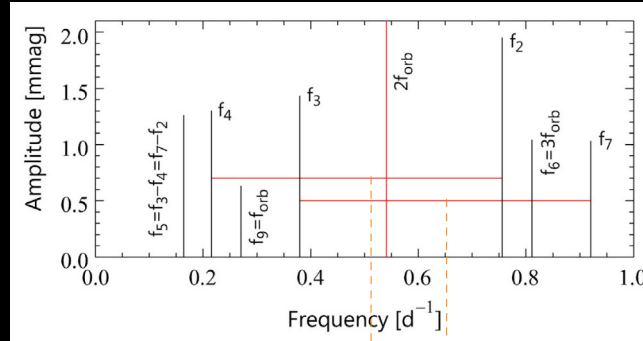
- Eclipsing binary consisting of B0.4IV and B0.7IV components (orbital period 3.89 days, slightly eccentric ~ 0.025 , apsidal motion with period of 72 years)
- TESS (two sectors; 2-min cadence): 9 significant frequencies \Rightarrow at least one component with β Cep pulsations



Tidal forces

→ π^5 Orionis (Jerzykiewicz et al., 2020, MNRAS 496, 2391)

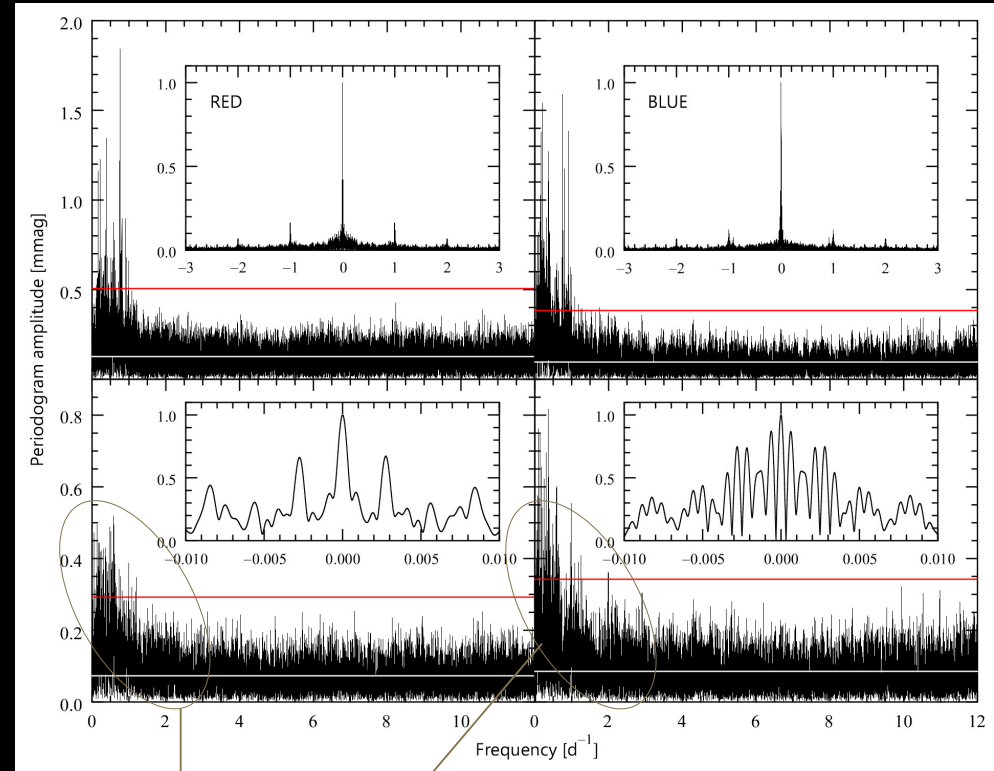
- SB1 system and ellipsoidal variable
- ✓ Two early B-type stars
- ✓ $P_{\text{orb}} = 3.70$ days
- ✓ Circularized orbit
- ✓ Synchronized rotation
- Frequency analysis
- ✓ 9 frequencies



$\delta_{n}^{(1,0)}$ $\delta_{n'}^{(1,0)}$

Self excited $(\ell, m) = (1, 0)$ g-modes in primary
that are distorted by equilibrium tide
(if axis of pulsating component is tilted)

BRITE photometry (6 seasons in 2013-2019; UBr, BTr, BHR, BAb, BLb)



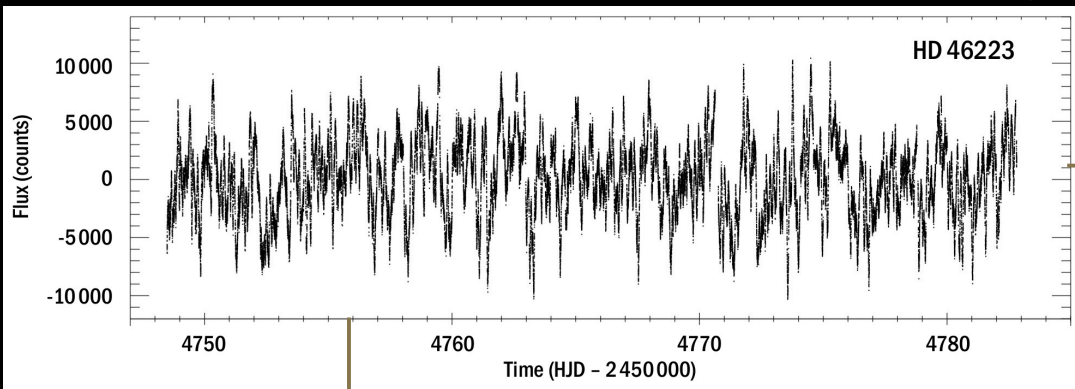
Red noise excess at low frequencies

Stochastic Low-Frequency Variability (SLFV)

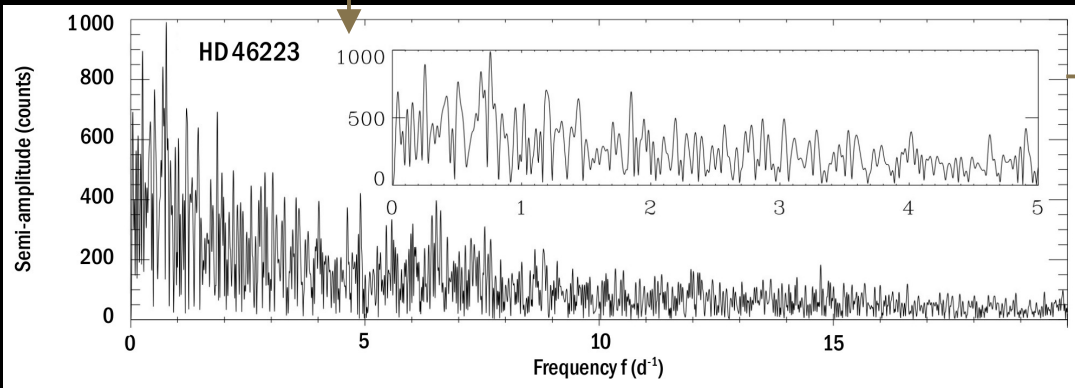
→ Observations of SLFV (red noise excess at low frequencies)

✓ Blomme et al., 2011, A&A 533, A4 → HD46223, HD46150 & HD4696 (O stars)

CoRoT



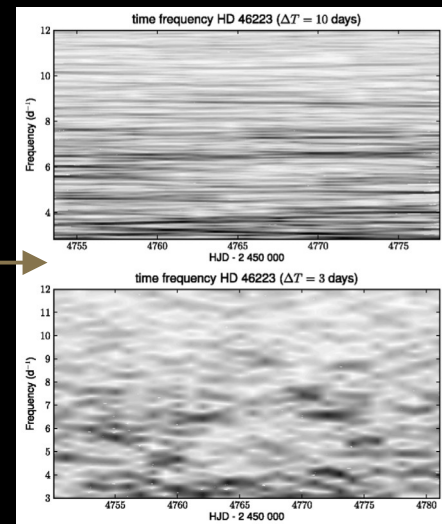
Lomb-Scargle periodogram



Time-dependent frequency analysis (sliding window)

Short-lived variability

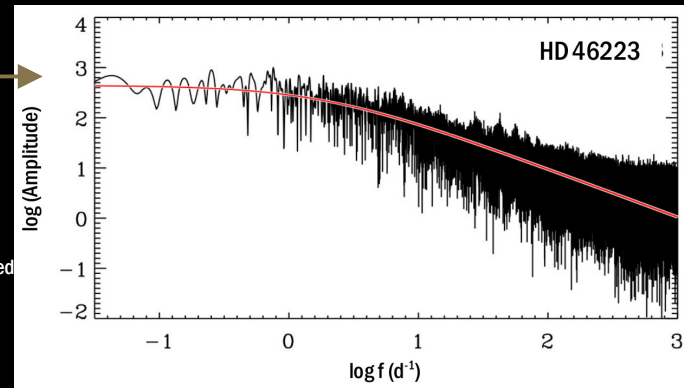
Stochastic excitation?



Semi-Lorentzian function

$$\alpha(f) = \frac{\alpha_0}{1 + (2\pi\tau_{\text{char}}f)^\gamma}$$

- with
- α_0 amplitude as $f \rightarrow 0$
 - τ_{char} characteristic timescale on which red noise is correlated
 - γ steepness of amplitude spectrum



Stochastic Low-Frequency Variability (SLFV)

→ Observations of SLFV (red noise excess at low frequencies)

✓ Blomme et al., 2011, A&A 533, A4	→ HD46223, HD46150 & HD4696 (O stars)	CoRoT
✓ Tkachenko et al., 2014, MNRAS 438, 3093	→ primary of massive binary V380 Cyg (B star)	Kepler + spectra
✓ Aerts et al., 2017, A&A 602, A32	→ HD188209 (O9.5 lab blue supergiant)	Kepler + spectra
✓ Simón-Díaz et al., 2018, A&A 612, A40	→ HD2905 (early-B supergiant)	spectra
✓ Bowman et al., 2019, A&A 621, A135	→ 35 OBAF stars	CoRoT
✓ Bowman et al., 2019, NatAs 3, 760	→ 114 ecliptic OB stars & 53 LMC OB stars	K2 + TESS
✓ Dorn-Wallenstein et al., 2019, AJ 878, 155	→ 6 LMC yellow supergiants & 2 LMC luminous blue variables	TESS
✓ Bowman et al., 2020, A&A 640, A36	→ 70 OB stars	TESS + spectra
✓ Dorn-Wallenstein et al., 2020, AJ 902, 24	→ 28 LMC yellow supergiants & 48 Galactic red supergiants	TESS
✓ Rauw et al., 2019, A&A 621, A15	→ HD149404 (massive post-Roche Lobe overflow system)	BRITE
✓ Nasé et al., 2021, MNRAS 502, 5038	→ 26 Wolf-Rayet stars & 8 luminous blue variables	TESS
✓ Lenoir-Craig et al., 2022, AJ 925, 79	→ 50 Galactic Wolf-Rayet stars	BRITE
✓ Elliot et al., 2022, MNRAS 509, 4246	→ P Cygni (luminous blue variable)	BRITE
✓ Bowman et al., 2022, A&A 668, A134	→ 30 OB stars	CoRoT
✓ Kołaczek-Szymański et al., A&A 659, A47	→ MACHO 80.7443.1718 (blue supergiant + late O-type dwarf)	TESS
✓ Dorn-Wallenstein et al., 2022, AJ 940, 27	→ 101 LMC and 25 SMC cool supergiants	TESS

Feature observed for many different types of massive stars!

Stochastic Low-Frequency Variability (SLFV)

→ Characterisation of SLFV (red noise excess at low frequencies)

➤ Amplitude spectrum fitting (frequency domain)

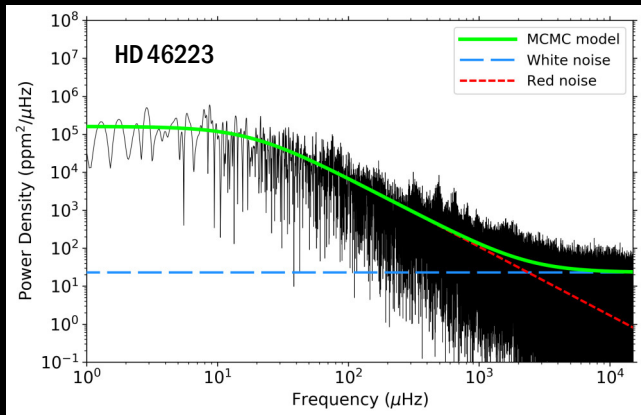
✓ Semi-Lorentzian function

- α_0 characteristic amplitude as frequency $\rightarrow 0$
- $\tau_{\text{char}} = 1/\nu_{\text{char}}$ characteristic timescale on which red noise is correlated
- γ steepness of amplitude spectrum
- α_w frequency independent noise term (white noise)

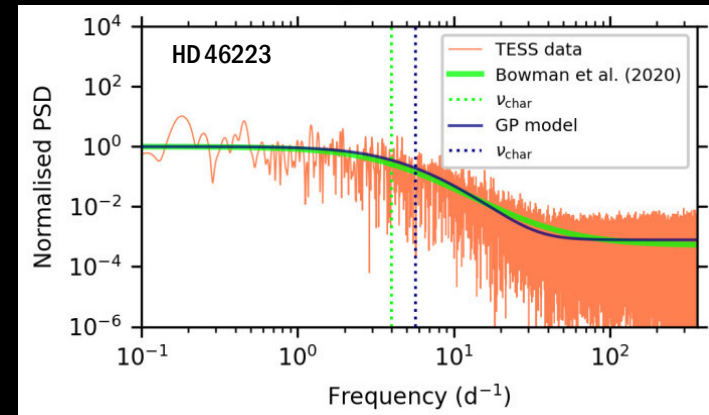
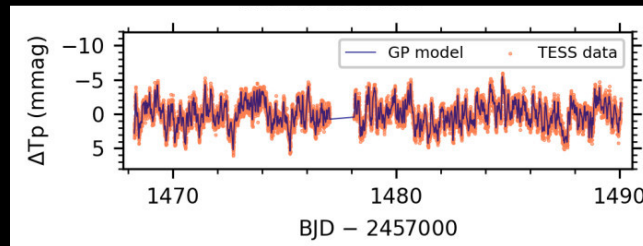
➤ Gaussian process regression (time domain)

✓ Damped simple harmonic oscillator

- σ_A characteristic amplitude
- $\rho_{\text{char}} = 2\pi/\omega_0$ characteristic variability timescale
- τ_{damp} characteristic damping timescale
- C_{jitter} jitter term to emulate uncorrelated noise in the observations
- Q quality factor (more damping if low value)



Bowman et al., 2019, A&A 621, A135



Bowman et al., 2022, A&A 668, A134

Stochastic Low-Frequency Variability (SLFV)

→ Characterisation of SLFV (red noise excess at low frequencies)

➤ Amplitude spectrum fitting (frequency domain)

✓ Semi-Lorentzian function

- α_0 characteristic amplitude as frequency $\rightarrow 0$
- $\tau_{\text{char}} = 1/\nu_{\text{char}}$ characteristic timescale on which red noise is correlated
- γ steepness of amplitude spectrum
- α_w frequency independent noise term (white noise)

➤ Gaussian process regression (time domain)

✓ Damped simple harmonic oscillator

- σ_A characteristic amplitude
- $\rho_{\text{char}} = 2\pi/\omega_0$ characteristic variability timescale
- τ_{damp} characteristic damping timescale
- C_{jitter} jitter term to emulate uncorrelated noise in the observations
- Q quality factor (more damping if low value)

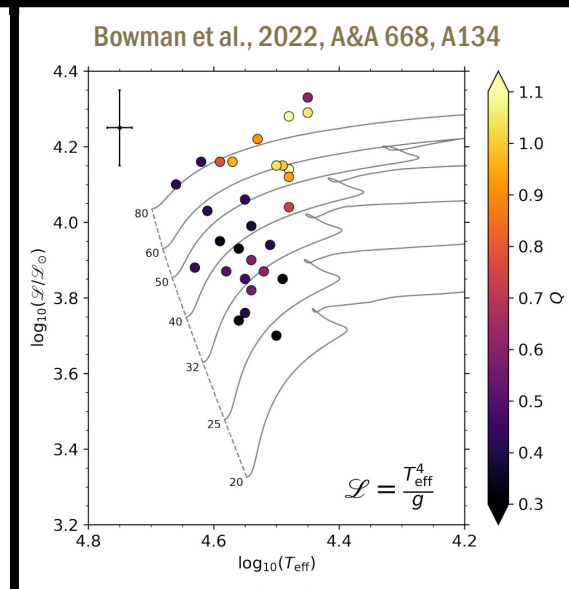
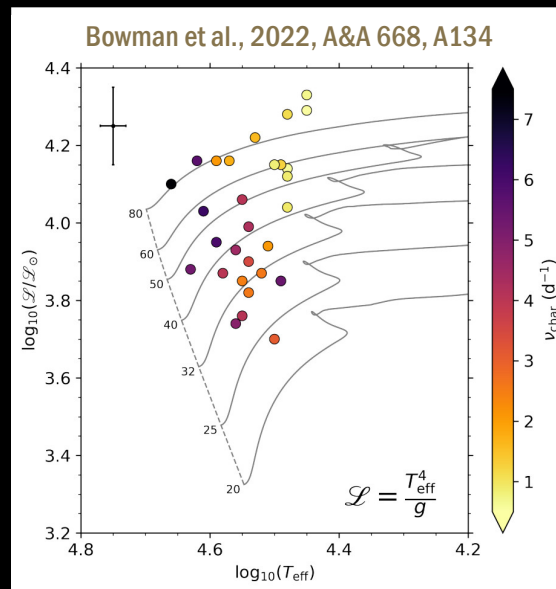
“yellow subgroup”:

- Low ν_{char} + high α_0/σ_A + low ν_{damp}
- Higher mass
- More evolved (closer to TAMS)
- Less stochastic (high Q value)

“blue subgroup”:

- High ν_{char} + low α_0/σ_A + high ν_{damp}
- Less evolved (closer to ZAMS)
- More stochastic (low Q values)

ν_{char} probes mass, age and
degree of coherency



Stochastic Low-Frequency Variability (SLFV)

→ Interpretation of SLFV

- **Surface granulations** (cf. red giant stars)
- **Internal Gravity Waves (IGWs)**
 - ✓ Travelling waves that are stochastically excited at the interface of a convective region and a stably stratified zone
 - turbulent core convection
 - turbulent pressure fluctuations in subsurface convective zones in outer envelope (Fe-opacity peak convection zone)
 - ✓ Propagate and dissipate within radiative regions
- **Wind-driven processes**
 - ✓ Clumpy, aspherical, and inhomogeneous stellar wind (line deshadowing instability)

Stochastic Low-Frequency Variability (SLFV)

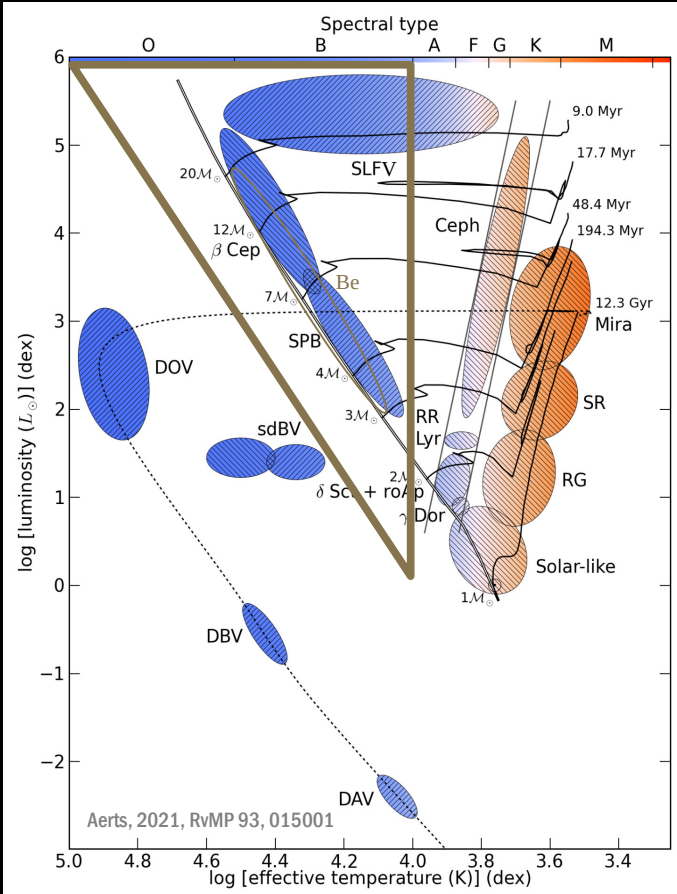
→ Interpretation of SLFV

- Surface granulations (cf. red giant stars) but v_{char} order of magnitude smaller than predicted v_{gran} for majority of stars (Bowman et al., 2019, A&A 621, A135)
- Internal Gravity Waves (IGWs)
 - ✓ Travelling waves that are stochastically excited at the interface of a convective region and a stably stratified zone
 - turbulent core convection
 - turbulent pressure fluctuations in subsurface convective zones in outer envelope (Fe-opacity peak convection zone)
 - ✓ Propagate and dissipate within radiative regions
- Wind-driven processes
 - ✓ Clumpy, aspherical, and inhomogeneous stellar wind (line deshadowing instability)

No consensus yet...

OB-type stars

Convective core
Radiative envelope



- β Cephei stars (β Cep)
- Low order p and g modes with periods of few hours
- Slowly Pulsating B stars (SPB)
- High order g modes with periods of several hours to few days
- Stochastic low-frequency variability (SLFV)
- α Cygni stars
- Fast Yellow Pulsating Supergiants (?)
- Be stars (Be)
- Pulsations
- Maia variables (?)

Hybrids!

Influencing factors

- Opacities
- Interior mixing profile
- Interior rotation profile
- Interior temperature profile
- Tidal forces
- Magnetic fields
- Mass loss
- Stellar wind

Excitation mechanisms at play

- Opacity mechanism operating in Z bump
- Stochastic excitation
- Non-linear mode excitation
- Rotation
- Tidal excitation

Peter De Cat (Royal Observatory of Belgium, Ringlaan 3, B-1180 Brussels, Belgium)

Group meeting at BNU (25/09/2024, Beijing, China)